—研 究 論 文—
Scientific Papers

New Ship-Borne Gravimeter NIPR-ORI Model II Installed on Board Icebreaker SHIRASE

Jiro SEGAWA[1], Katsutada KAMINUMA[2], Hiroaki TOH[1], Yoichi FUKUDA[1] and Chul Soo YANG[1]

砕氷船「しらせ」に搭載された船上重力計 NIPR-ORI II 型

瀬川爾朗[1]・神沼克伊[2]・藤　浩明[1]・福田洋一[1]・梁　哲寿[1]

要旨: 日本南極地域観測隊で使用される新しい船上重力計 NIPR-ORI II 型について述べる．この重力計は NIPR-ORI I 型の改良型であり，慣性航法級の tuned dry gyro (TDG) が使われている．1987 年に東京大学海洋研究所の白鳳丸によって，最初のテストが行われ，船速によるエトベス効果の補正をした後の最終的な観測精度は ±0.5 mgal よりも良いことが確かめられた．

Abstract: A newly-designed ship-borne gravimeter NIPR-ORI Model II to be used for the Japanese Antarctic Research Expedition is described. This meter is a second version of the previously used NIPR-ORI Model I. The new gravimeter is equipped with the inertial grade gyro called TDG (tuned dry gyro). The first performance test was conducted on board the R/V HAKUHO MARU of the Ocean Research Institute, University of Tokyo in 1987, and it was found that the overall accuracy of the meter after the correction for the Eotvos effect caused by ship's speed was better than ±0.5 mgal.

1. Introduction

The NIPR-ORI ship-borne gravimeter was first developed in 1980 under a cooperation between National Institute of Polar Research and Ocean Research Institute, University of Tokyo. This meter was designed on the basis of the following principles:

1) Employment of a servo-accelerometer for the sensor which is linearly related to acceleration. The servo-accelerometer has a rugged structure.

2) Separation of the vertical gyroscope from the sensor platform which exactly follows up the gryo.

3) Employment of a 32-bit mini-computer which processes gravity and navigational data in real time.

The NIPR-ORI gravimeter Model I manufactured in this way was used on board the Japanese icebreakers FUJI and SHIRASE for the Japanese Antarctic Research Expeditions from 1980 to 1987 (KASUGA *et al.*, 1983; SEGAWA *et al.*, 1983, 1986).

In 1986 the NIPR-ORI gravimeter Model II was designed and manufactured. The design principles of the NIPR-ORI Model II which were decided on the basis of the experiences from Model I were as follows:

[1] 東京大学海洋研究所. Ocean Research Institute, University of Tokyo, 15–1, Minamidai 1-chome, Nakano-ku, Tokyo 164.

[2] 国立極地研究所. National Institute of Polar Research, 9–10, Kaga 1-chome, Itabashi-ku, Tokyo 173.

1) Employment of a servo accelerometer which is specially designed for gravity sensor so that it has higher sensitivity and stability.

2) Employment of a Schuler-tuned vertical gyroscope which is unaffected by ship's maneuvers.

3) Employment of a 32-bit super mini-computer with a hard disc and magnetic tape memories for processing gravity and navigational data.

2. Outline of the Gravimeter System

The new NIPR-ORI gravimeter Model II is composed of the units listed in Table 1. The combination of the units is essentially the same as Model I, but their specifications have been graded up.

Figure 1 shows a photograph of the assembled NIPR-ORI gravimeter Model II and Fig. 2 shows the schematic picture of the assembly. It has become two-thirds in size and weight as compared with that of the previous model. In Table 2 is listed the weight of the units.

Figure 3 shows a block diagram of the system of NIPR-ORI gravimeter Model II. Voltage output from the gravity sensor is compared with the precise reference voltage with the stability of 3 μV over the range of 30 V and the difference between the two outputs, *i.e.*, sensor voltage minus reference voltage, is introduced to a digital

Table 1. Units and specifications of the NIPR-ORI gravimeter Model II.

Time code generator	·Year, month, day, hour, min, s ·Timing pulse output: 10, 50, 100, 200 ms ·Relative accuracy 10^{-10} Absolute accuracy 10^{-6}
Gravity sensor	·Servo accelerometer with flexible hinges ·Range of linear response $\pm$G ·Resolution 0.01 mGal ·Sensitivity 30 μV/mGal ·Response frequency DC $\sim$30 HZ
Gravity sensor control	
Vertical gyroscope (VG-120)	·Tuned Dry Gyro (TDG) ·Schuler synchronization ·Roll angle $\pm$40° ·Pitch angle $\pm$20° ·Verticality $\pm$ 3′ ·Stabilization time 2 hours
Vertical gyroscope control	
Stabilized platform (SP-120)	·Gyro follow-up system with DC servo torquers ·2×, 36× synchro transmission ·Static follow-up accuracy $\pm$15″ ·Dynamic follow-up accuracy $\pm$1.5′ under the conditions Roll $\pm$20°, 8 s Pitch $\pm$5°, 6 s Yaw $\pm$5°, 10 s ·Maximum load allowable 12 kg

Table 1. (*Continued*).

Stabilized platform control	
Gyrocompass (SR-220)	·Accuracy $\pm 0.5°$ ·Roll, Pitch $\pm 45°$
Digital voltmeter	·FLUKE 8505A multimeter ·Full scale 6 1/2 digits or 7 1/2 digits ·Resolution 1 μV with 2 V range ·Input resistance 10000 MΩ ·Accuracy 8×10^{-6}/24 h 15×10^{-6}/90 days at 2 V range ·Zero stability <5 μV/90 days
Data processing unit	·Data General Eclipse 4000 DC ·Word length 32 bits ·Cycle time 200 ns ·Main memory 8 Mbytes ·Disc capacity 240 Mbytes ·Address space 4 Gbytes ·Printer ·Magnetic tape unit ·Display console ·Photo driver unit ·Interface to input navigational data
Shock absorbing board	·Air cushion ·Resonant frequency lower than 5 Hz

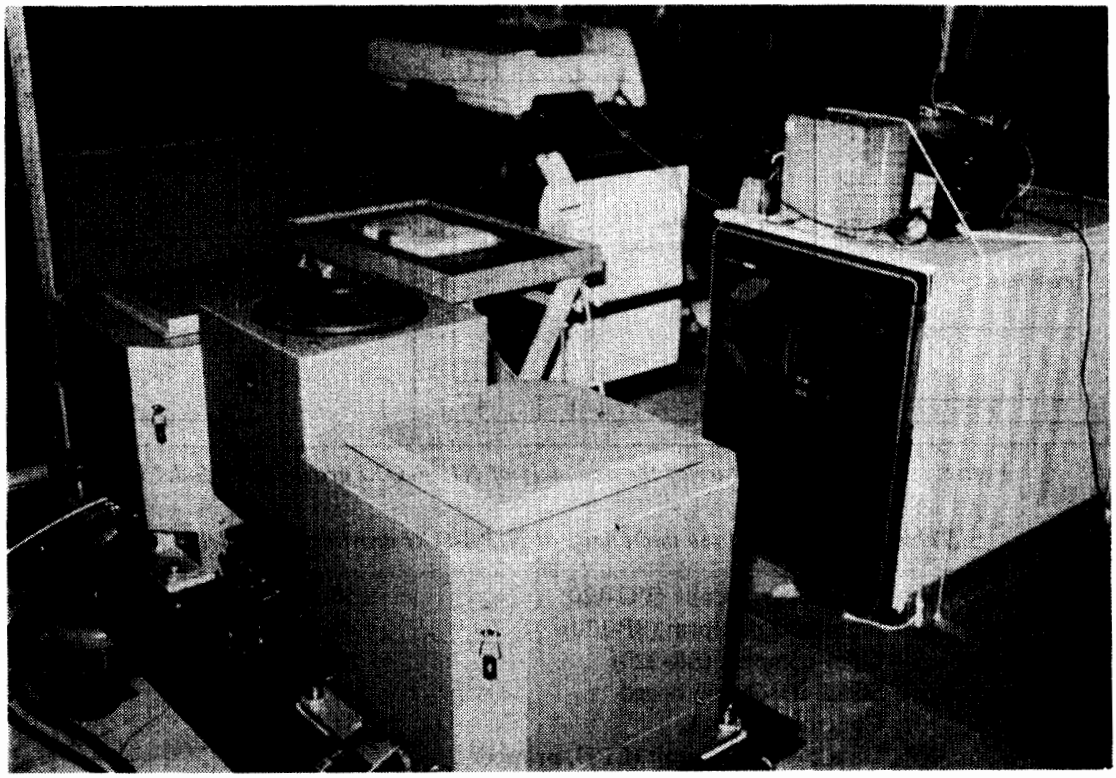

Fig. 1. NIPR-ORI gravimeter Model II.
This shows vertical gyro, gravity sensor platform and 32-bit super mini-computer. The control electronics units are not shown here.

voltmeter for AD conversion. The conversion is conducted with a resolution of 1 μV which corresponds to 0.033 mgal, at the interval of either 10, 50, 100 or 200 ms. The gravity sensor is mounted on the stabilized platform which is driven by direct DC servo torquers. The vertical gyroscope is a Schuler-tuned dry gyro with two degrees

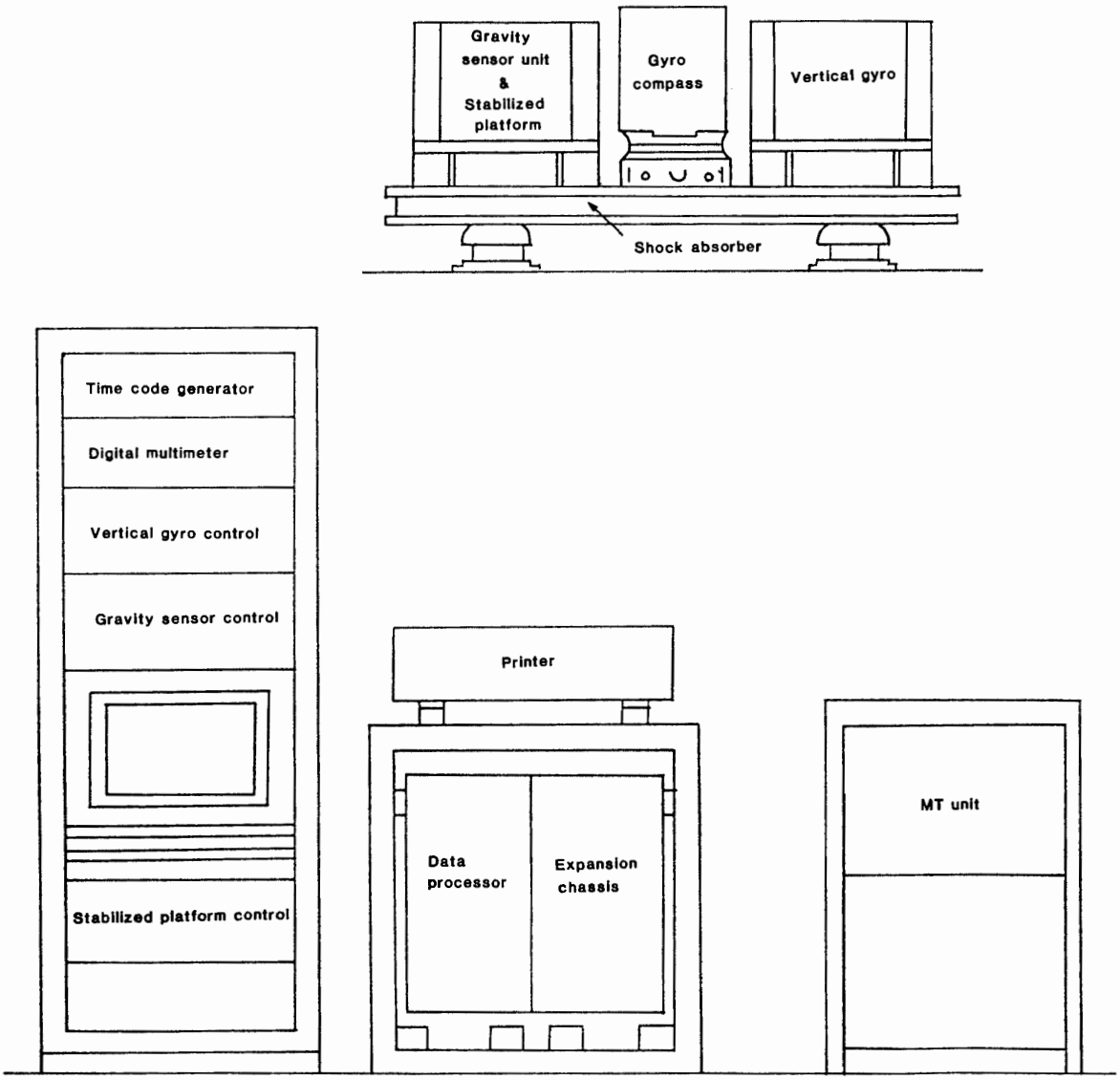

Fig. 2. A schematic picture of the assembly of NIPR-ORI gravimeter Model II.

Table 2. Weight of the main units of NIPR-ORI gravimeter Model II.

Vertical gyroscope (VG-120)	50.5 kg
Stabilized platform (SP-120)	49.5 kg
Gyro compass (SR-220)	35.5 kg
Shock absorbing board	249.5 kg
Control unit rack	254.5 kg
Data processing unit (CPU, printer)	193.5 kg
Magnetic tape unit	68.5 kg
Photo driver unit	7.5 kg
Sum	909.0 kg

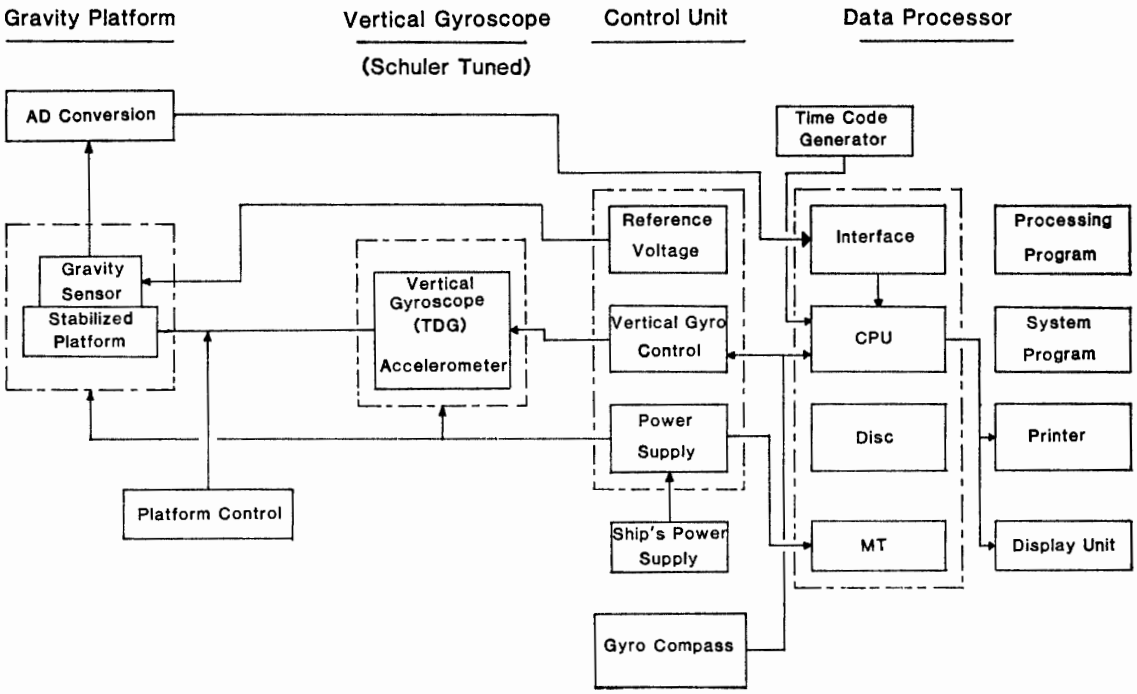

Fig. 3. Block diagram of the NIPR-ORI gravimeter Model II system.

of freedom. The gyrocompass provides the vertical gyro and the data processing unit with the ship's heading information which is necessary to control the vertical gyro and to correct the gravity data. The time code generator provides the time reference. The data processing unit processes and stores the gravity signals together with navigational information.

3. Gravity Sensor

Figure 4 shows the design of the gravity sensor and Fig. 5 shows its housing. The sensor is 80 mm in diameter and 45 mm high. The proof mass is suspended by a flexible hinge on one end and a pick-up coil is attached to on the other end. There is a stopper above and below the proof mass/horizontal beam, so that the beam may not be deflected too much. About the center of the horizontal beam are installed a pair of coils, which are sandwiched between a pair of permanent magnets from the above and below. The coils and magnets compose a vertical torquer which compensates for vertical acceleration. The important points in designing the sensor are the pendulosity of proof mass and the stability of the magnet. Pendulosity of proof mass is related to response speed of the pendulum and the sensitivity. The servo accelerometer in general has been designed to have relatively small pendulosity for the sake of increasing ruggedness. This requirement was from the air and space use in controlling the spacecraft. As the gravity sensor the servo accelerometer must have sensitivity and stability much higher than those for the other use. So, the present gravity sensor has a higher pendulosity at the cost of response speed and ruggedness. The maximum response speed of this sensor is 30 Hz, which is regarded so slow among the similar accelerometers for air and spacecraft. The permanent magnet has generally a large drift and tem-

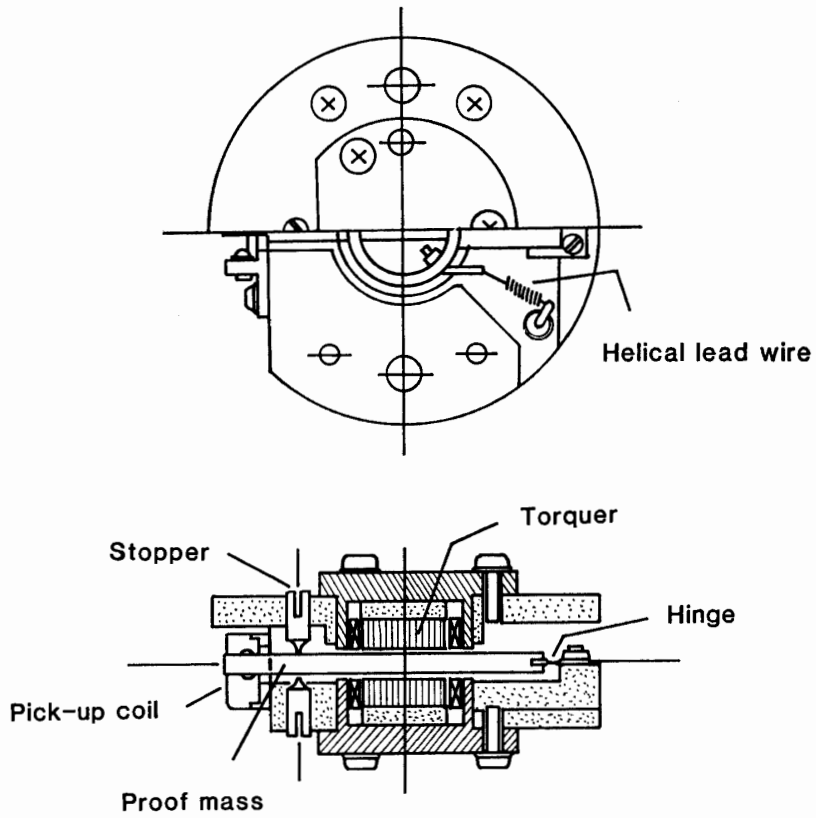

Fig. 4. Brief design of the gravity sensor.

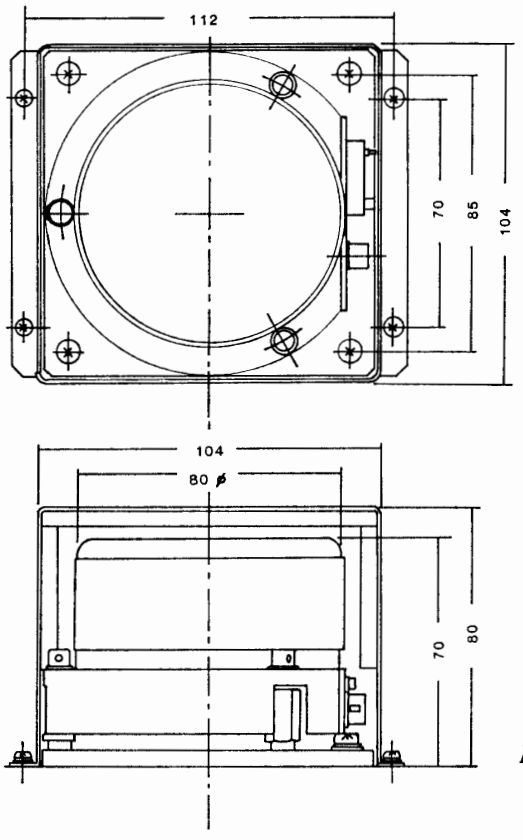

Fig. 5. Housing of the gravity sensor with double casings. The inner case is hermetically sealed.

perature change of magnetization. Drift rate of magnetization with time depends on the material and the method by which it is magnetized. Drift rate is also related to the ambient temperature. Magnet used for the present sensor is made of rare earth material. After a necessary annealing treatment the drift rate becomes extremely small. The temperature change of the sensor sensitivity is about 50 ppm/degree. The temperature inside the sensor housing is regulated at 45°C and kept constant within $\pm 1/1000$°C. The sensor housing which is evacuated is surrounded by a heater winding whose electric current is proportional to deviation of temperature. The housing of the stabilized platform is also regulated at temperature of 40°C$\pm$0.1°C.

In the case of the previous model the sensor housing was filled with viscous liquid. Although the viscous liquid is useful for damping, its bouyancy varies with temperature and its convective motion affects the balance of the proof mass. The sensor housing shown in Fig. 5 has double casings: The inner case is hermetically sealed, wound by a heating wire and thermally insulated. The outer case is also thermally insulated, cubic-shaped with sides of 112 mm$\times$112 mm$\times$80 mm.

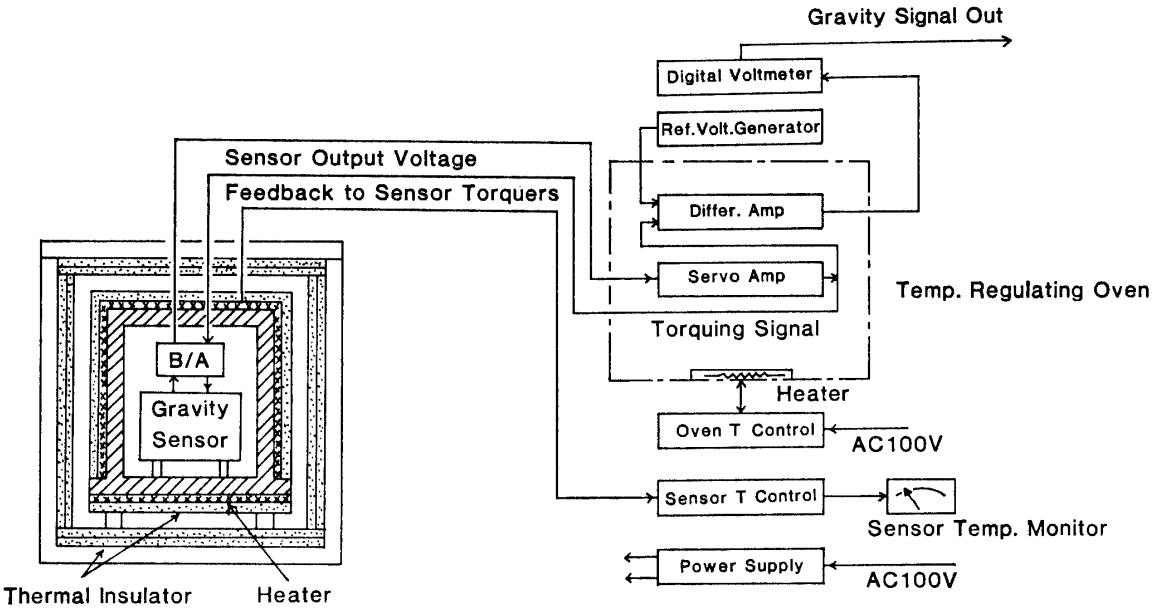

Fig. 6. Block diagram of gravity sensor control unit.

Figure 6 shows a block diagram of the gravity sensor control unit. The sensor generates an output voltage which is proportional to the movement of the pick-up coil from the center. This voltage is amplified and fed back to the torquing coils of the sensor. There is a buffer circuit inside the sensor to transmit and receive the signals. These feedback circuit functions to nullify the position of the proof mass. The torquer signal is proportional to gravity: To measure the torquer signal is to measure gravity. Therefore, the output from the servo amplifier is introduced to a precise differential amplifier which amplifies the difference voltage between the output voltage of the servo amplifier and the precise reference voltage. The output from the differential amplifier is proportional to gravity minus reference gravity. This output is digitized by a seven and one half-digit digital voltmeter. The gravity sensor servo amplifier

and the differential amplifier are housed in a temperature regulated oven which is kept at 50°C±0.1°C.

4. Vertical Gyroscope

The vertical gyroscope is a Schuler-tuned dry gyro. The tuned dry gyro (TDG) is one of the newest type gyroscope with two degrees of freedom. The reason why this type of gyroscope was employed is that it is immune from the maneuvers of a ship so that it can give a correct vertical reference even when a ship is turning. The conceptional picture of the tuned dry gyro is shown in Fig. 7. A flywheel is connected to a gimbal ring by means of flexible hinges and the gimbal ring is in turn connected to the shaft of a motor by means of other flexible hinges that are perpendicular to the former. The gimbal ring works as a kind of universal junction. The flywheel rotates at a high speed to acquire a large angular momentum. The flexible hinge has a nature that it can be twisted very softly and yet it cannot be bent easily. With this structure the flywheel of TDG does not change the spin axis even if the motor shaft inclines, so that it is possible to detect the deflection of the motor shaft with respect to the flywheel. When the motor shaft inclines an undesirable vibratory motion occurs to the gimbal ring, which has the same period as that of the rotation of motor. This vibration causes precession of the flywheel. If the angular velocity of motor is ω, the moment of inertia about the inner and the outer hinges a, and the moment of inertia about the motor shaft c, then the torque T that causes the precession is approximately given by

$$T=\left(-a+\frac{1}{2}c\right)\omega^2\alpha\ ,$$

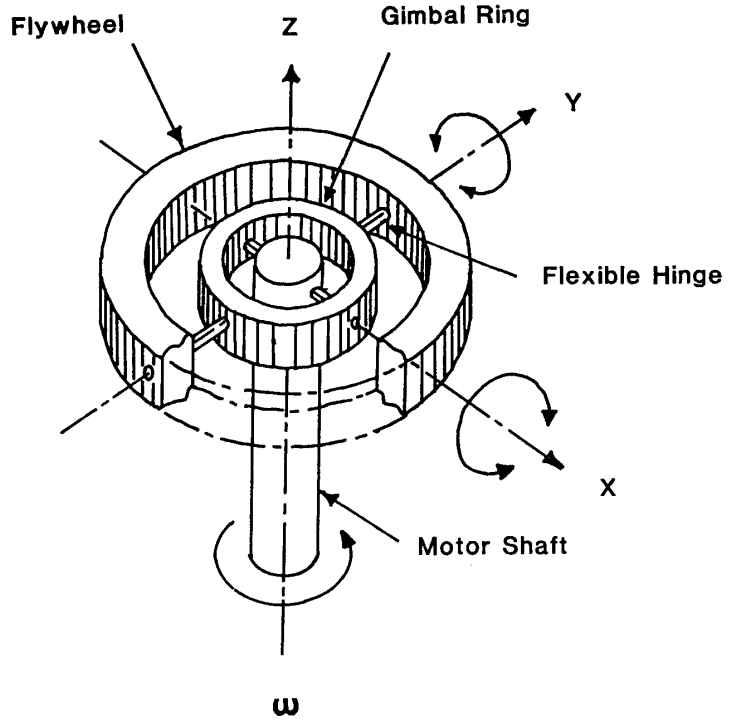

Fig. 7. Conceptional picture of tuned dry gyro.

where α is inclination of motor shaft. This kind of torque is not desirable for a gyro, and so various means is taken so that T becomes zero. If $a=(1/2)c$, then $T=0$. But this condition is difficult to attain. It is usually taken to reduce the torque that the intrinsic elasticity of the flexible hinge is adjusted and utilized so that the torques caused

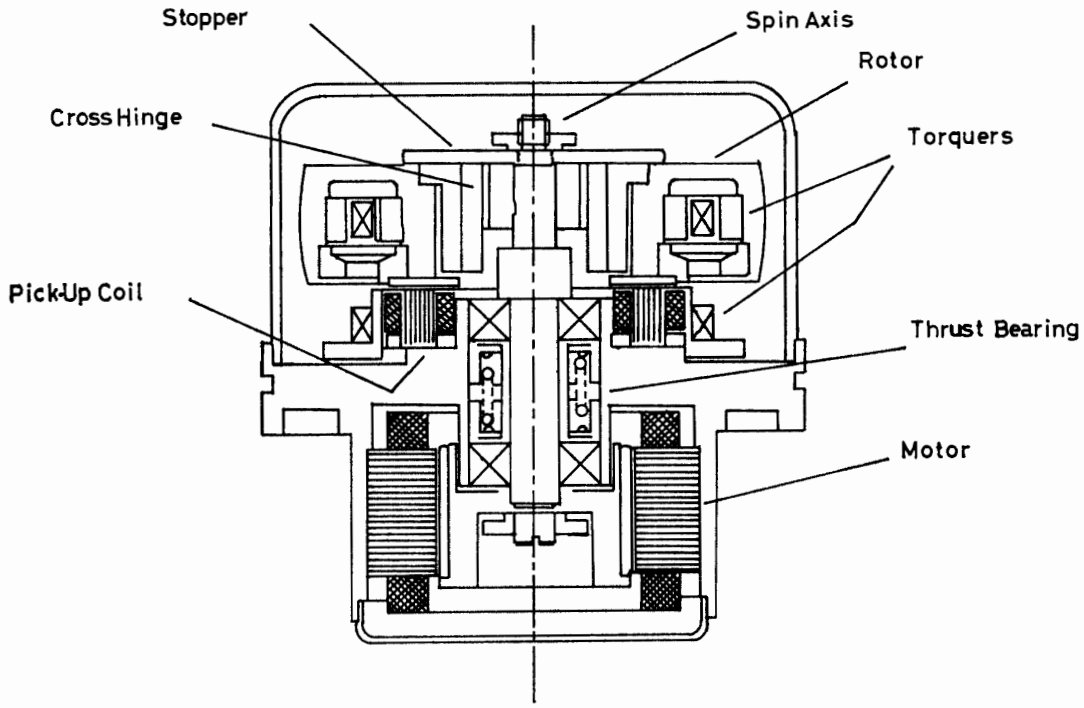

Fig. 8. Design of tuned dry gyro used for this gravimeter.

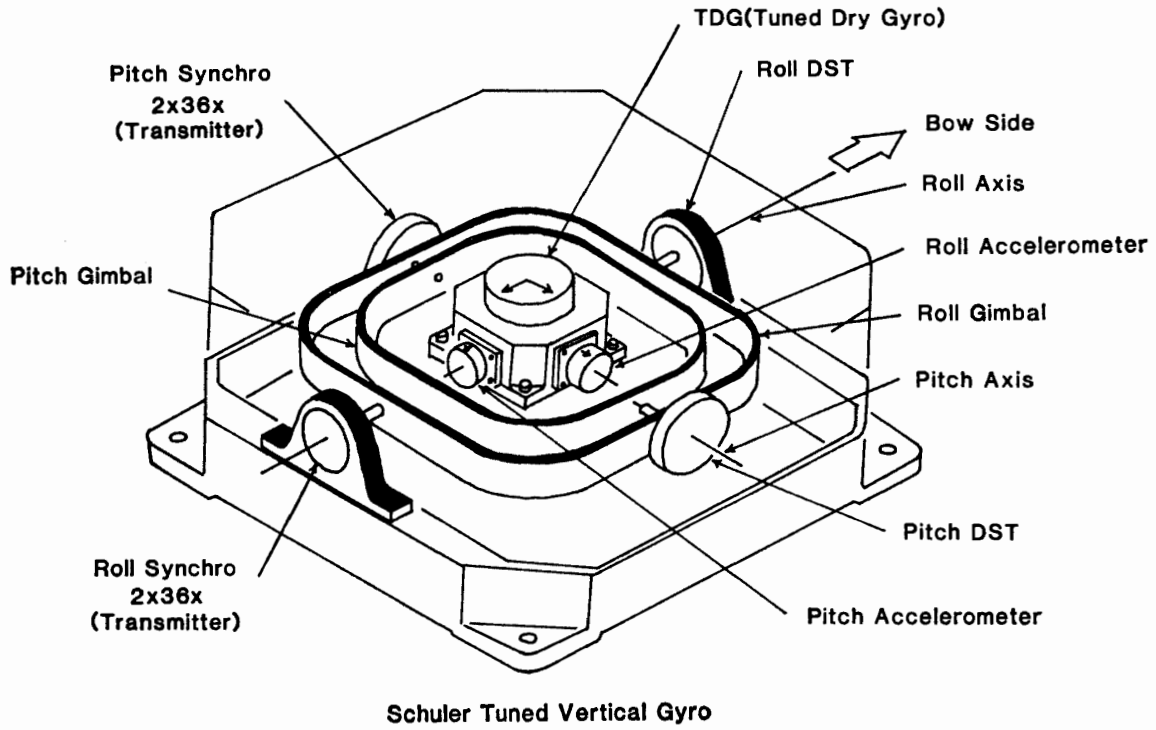

Fig. 9. Schematic picture of vertical gyroscope.

by vibration and the elasticity may cancel each other. This is called torque tuning. The TDG gyro shows generally a good quality. The gyro drift is usually as small as 0.01°/hour.

Figure 8 shows the design of TDG gyro used for this gravimeter. The flywheel (rotor) is connected to the motor shaft through cross hinges. Deflection of flywheel relative to the motor shaft or the gyro base is detected by pick-up coils which are placed beneath the flywheel. Gyro torquers to cause precession on the spinning flywheel are installed inside and outside of the flywheel.

Figure 9 is a schematic picture of the vertical gyroscope. TDG gyro is mounted on gimbals which consist of a pitch and a roll gimbal. Both gimbals are equipped with horizontal (roll and pitch) servo accelerometers, direct servo torquers (DST) and synchro transmitters (2x, 36x). Horizontal servo accelerometers sense inclination of the gimbals plus ship's horizontal acceleration. Then the signals from the horizontal accelerometers are amplified and fed to torquers of the TDG gyro which cause the precession of the flywheel in such a fashion as the horizontal accelerometers level. The flywheel of TDG is somewhat deflected with respect to the base of TDG, so that the pick-up coils installed inside TDG output error signals to DST attached to the pitch and roll gimbals. The DST corrects the attitude of the gimbals in a sense that the output from the pick-up coils is reduced. During this feedback operation the flywheel of TDG aligns the vertical to which the pitch and roll gimbals exactly line up.

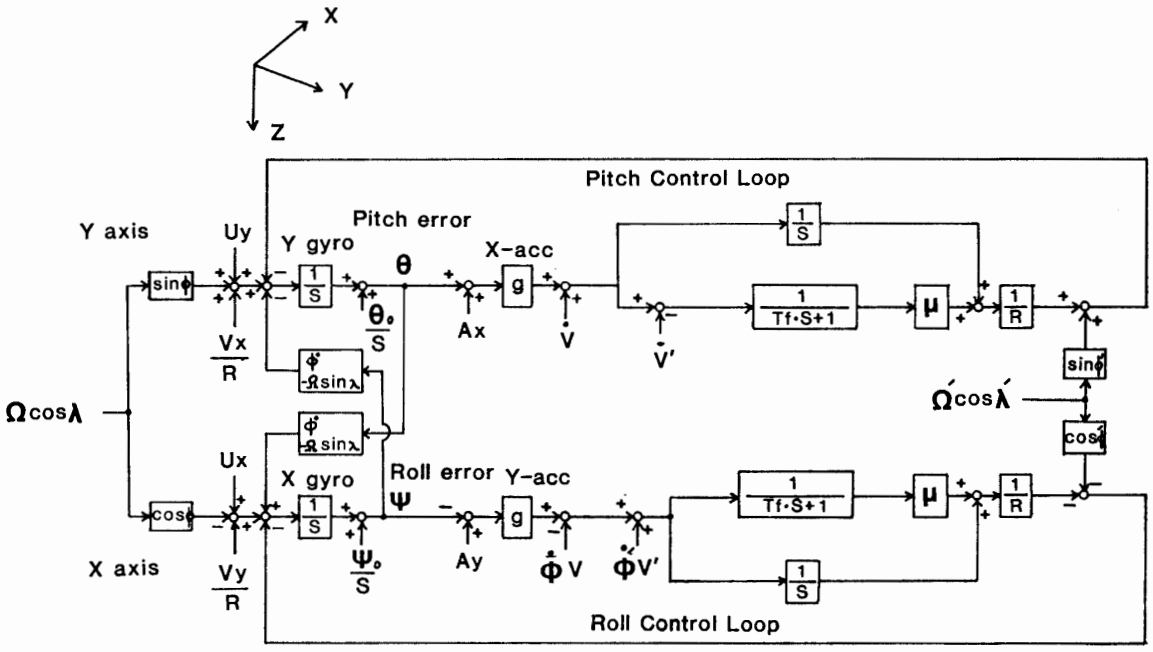

Fig. 10. Block diagram of the feedback loop to control the Schuler-tuned gyro.

θ, θ_0: *Pitch error and its initial value.*
ψ, ψ_0: *Roll error and its initial value.*
ϕ: *Ship's heading.*
Ω: *Angular velocity of the earth's rotation.*
g: *Gravity.*
R: *Mean radius of the Earth.*
V_x, V_y: *Ship's velocity in the x and y directions.*
U_x, U_y: *Gyro drift in the x and y directions.*
A_x, A_y: *Biased acceleration in the x and y directions.*
T_f: *Time constant of filter.*
μ: *Damping constant.*
$\cdot$: *Derivative with respect to time.*
$'$: *Estimated value or estimated correction.*
S: *Laplace operator.*
λ: *Latitude.*

Figure 10 is a block diagram of the feedback loop which is employed in the Schuler-tuned gyro. The upper part of the diagram is the loop for pitch control, and the lower for roll control.

Suppose the rectangular co-ordinates x, y and z are taken fore, athwartships and downwards, respectively. Then, the pitch angle of a gyro is made by the rotation about y axis and the roll angle by the rotation about x axis. Let the deflection of a gyro from the vertical be denoted by θ and ϕ, which show a pitch error that is the deflection of the gyro about y axis and a roll error that is the deflection of the gyro about x axis, respectively. The deflection of the gyro is caused mainly by five factors, *i.e.*, initial offset angle of the gyro, rotation of the earth, drift of the gyro, cruising of the ship and change of the ship's heading.

Let's discuss the characteristics of the feedback loop with respect to the pitch control loop, because the roll control loop can be discussed similarly. The component of the earth's rotation vector in y direction is expressed by $\Omega \cos\lambda \sin\phi$ where Ω is angular velocity of the earth's rotation, λ is latitude of the ship and ϕ is heading of the ship. An uncontrolled ideal gyro is deflected off the vertical with the rate of $\Omega \cos\lambda \sin\phi$ about the y axis. A gyro is actually subject to intrinsic drift with a rate of U_y due to imperfection of the mechanism. Also, when the ship cruises with a speed of V_x, it generates the change of the vertical with the rate V_x/R where R is the mean radius of the earth. The other factors that cause deflection of the gyro from the vertical is the secondary effect from the z component of the earth's rotation vector as well as the change of the ship's heading. Since the rotation vector about z axis is perpendicular to x and y axes, it should have no effect on pitch and roll errors. But, once there should exist pitch or roll error, the z component of the earth's rotation vector and/or the change of the ship's heading cause cross coupling errors on the pitch or roll angle: the pitch error θ causes the roll error with the amount of $\theta(\dot{\phi}-\Omega\sin\lambda)$ and the roll error ϕ causes the pitch error with the amount of $\phi(\dot{\phi}-\sin\lambda)$, when $\dot{\phi}$ is the rate of the ship's heading change and $-\Omega\sin\lambda$ is the z component of the earth's rotation vector.

All the factors of the deflection of the gyro cause torques on the y gyro or the x gyro (or y or x axis of a gyro with two degrees of freedom) through accelerometers and torquers. In this case the gyro works as an integrator which is expressed by $1/S$ in terms of transfer function, where S is the variable of Laplace transform. As a result from this process we get the pitch error θ including the initial offset angle θ_0. The pitch error θ is sensed by the x-accelerometer installed on the x axis. The x-accelerometer involves some amount of bias error denoted by A_x. The x-accelerometer also senses the change of the ship's speed $\dot{V}$. Therefore, the total output of the x-accelerometer is expressed by $(A_x+g\theta+\dot{V})$. The change of the ship's speed can be estimated by calculation using the ship's speedometer such as the electromagnetic log. Let the estimated speed be denoted by $\dot{V}'$, and it is subtracted from the output of the x-accelerometer. The signal $(A_x+g\theta+\dot{V}-\dot{V}')$ is introduced into two lines: In one line it is integrated with time electronically as seen by the transfer function $1/S$. In the other line it is low-pass-filtered with a time constant T_f. The transfer function of the low pass filter is $(T_fS+1)^{-1}$ which is regarded as a damping factor μ of the signal $(\mu=(T_fS+1)^{-1})$. The integrated signal and the damped signal are added together to

make a modified x acceleration sensed by the x-accelerometer. This output is again divided by R to be converted to the pitch error angle. The component of the earth's rotation vector can be calculated using latitude and ship's heading provided by the ship's navigational device. It is expressed by $\Omega \cos\lambda' \sin\phi'$ with respect to y axis. The calculated component of the earth's rotation is added to and fed back to the y gyro. In this stage the loop is closed. The similar process can be followed with the case of the roll control loop. The ship's acceleration in the y direction (athwartships) occurs by ship's yawing and it is expressed by $\dot{\phi}V$ or $\dot{\phi}'V'$.

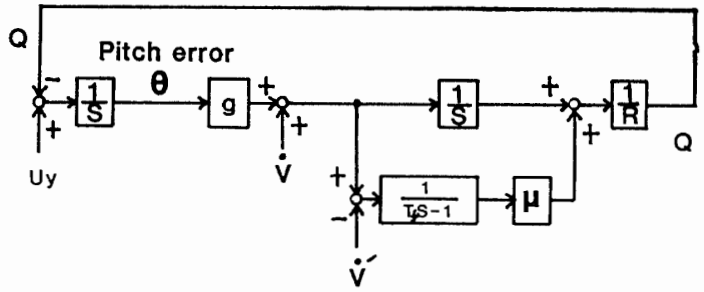

Fig. 11. Simplified block diagram of the feedback loop to control the Schuler-tuned gyro. Notations are the same as in Fig. 10.

When the calculated components of the earth's rotation vector exactly coincide with the actual ones and the secondary effect on the deflection of the gyro from the earth's rotation is neglected, the control loop of Fig. 10 can be simplified as shown in Fig. 11. Suppose the feedback signal be denoted by Q. Then, the pitch error θ, for instance, is expressed by equation

$$\theta=\frac{U_y-Q}{S}\ .$$

On the other hand, Q is expressed by

$$Q=\frac{(g\theta+\dot{V}-\dot{V}')\frac{1}{S}+(g\theta+\dot{V}-\dot{V}')\mu}{R}\ ,$$

when

$$\mu=\frac{1}{T_fS+1}\ .$$

If the above two equations are combined we get

$$\theta=\frac{U_y}{S}-\frac{(g\theta+\dot{V}-\dot{V}')\left(\frac{1}{S}+\mu\right)}{RS}\ ,$$

$$\therefore\quad \theta=\frac{SU_y-(1+\mu S)\frac{\dot{V}-\dot{V}'}{R}}{S^2+\frac{g}{R}\mu S+\frac{g}{R}}\ .$$

when the characteristic equation is expressed by

$$S^2+2\xi\omega_0 S+\omega_0{}^2=0 ,$$

then

$$\omega_0=\sqrt{\frac{g}{R}} ,$$

$$\xi=\frac{\mu\omega_0}{2} .$$

The fundamental period of this feedback loop T_0 is

$$T_0=\frac{2\pi}{\omega_0}=84.4 \text{ min} ,$$

which is known as Schuler period.

In this way the Schuler-tuning of the gyro is realized, and the TDG behaves like a long period damped pendulum with a period of 84.4 min. The feedback loop to control TDG is regulated by CPU INTEL 8086. The signals from the roll and pitch accelerometers and synchro transmitters are all digitized and input to CPU. The CPU acquires information of ship's speed and heading and calculates the ship's position (latitude and longitude). Using all the information the CPU estimates the quantity of the feedback signal to torquers of TDG. The calculated latitude, longitude, ship's speed and heading, and the digitized ship's accelerometers (cm/s^2) and the amount of torquing power (deg/H) can be read on the liquid crystal display (LCD) at the front panel of the vertical gyro control. Corrections of these values or resetting them can be made manually from keyboard. By the LCD can be monitored the situation of TDG operation. When TDG is started the LCD displays 'initial mode'. When the gyro is being stabilized the display is changed from 'leveling mode', 'alignment mode' and finally to 'navigation mode'. It takes almost 2 hours for TDG to become sufficiently stable. The LCD displays alarms when there is a failure. They are 'Log failure', 'Gyro failure', 'Pick-up failure', 'Rotor failure', 'Temperature failure' and 'Servo failure'.

5. Stabilized Platform

Figure 12 shows a schematic picture of the stabilized platform with the gravity sensor mounted on it. The gimbals are exactly the same as those used for TDG. Both the pitch and the roll gimbals are equipped with synchro receivers (2x, 36x) and DST's.

Figure 13 shows a block diagram of platform control. Roll and pitch signals are given by TDG's synchro transmitter. The signals are received by the synchro receivers of the platform and the difference of level between the gyro and the platform is compared. If there is any difference, it is sent to the pitch and roll servo amplifiers as a follow-up error signal to drive DST's of the platform. The platform follows the attitude of TDG exactly within the deviation of ± 15 s of arc in static environment and ± 1.5 min of arc in dynamic environment. The follow-up error signals are displayed by analog voltmeters with a range of ± 10 min of arc. In order to have the gravity sensor exactly aligned vertical, the level of the platform can be adjusted manually using manual potentiometers. This adjustment can be made when the ship is

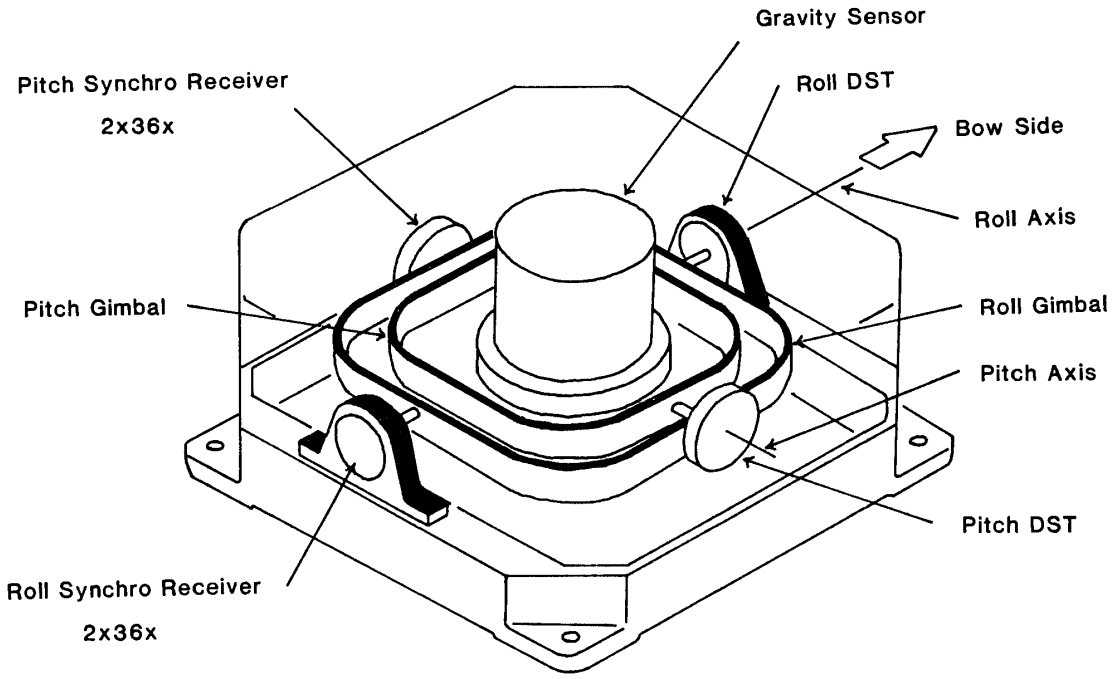

Fig. 12. Schematic picture of stabilized platform with the gravity sensor mounted on it.

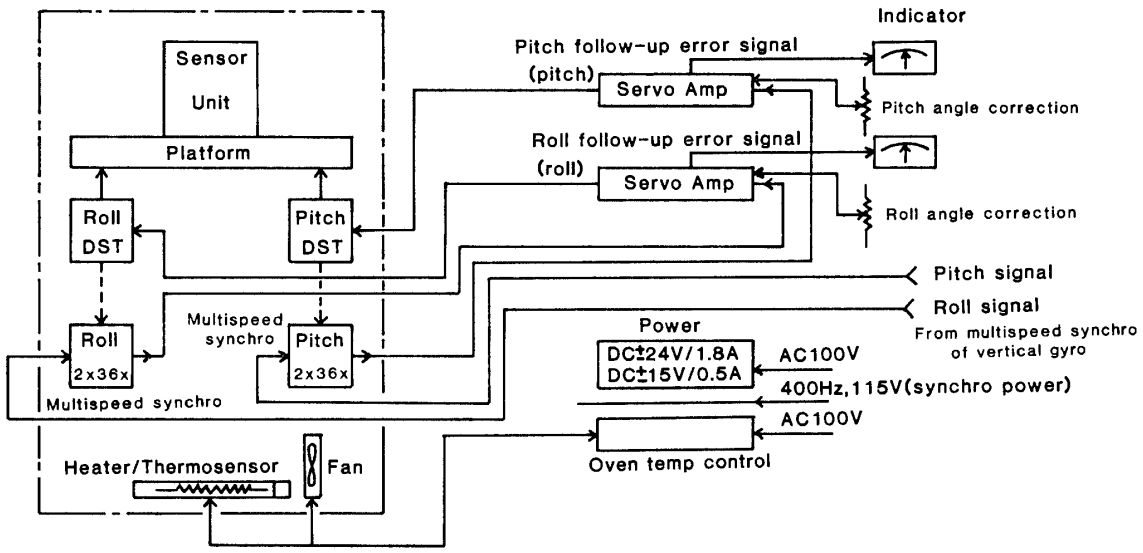

Fig. 13. Block diagram of platform control.

moored at a pier so that the gravity value becomes maximum. This platform is housed in a box whose temperature is kept at 40°C±0.1°C.

6. Data Processing Unit

The data processing unit consists of Eclipse 4000DC computer with a hard disc, and a magnetic tape unit, a printer unit and a strip-chart recorder for profiling gravity

change. In comparison with the computer (Nova III) previously used this computer can process a greater amount of data at a higher speed so that it becomes possible to sample data at a higher speed and to apply a longer filter. This capability is very important to enhance the accuracy of measurement.

The gravity signal from the sensor is digitized by a digital voltmeter and sent through the interfacing circuit to CPU of the Eclipse computer. The navigation information, time, ship's position, speed, heading and water depth are taken through interfaces and photo-driver and receiver units. Such photo couplers become necessary because the terminal of navigational data is remote from the room of the gravimeter and the unstability of electric potential of the ship's ground is suspected to occur.

7. Data Processing

Signals from the gravity sensor are read every 10, 50, 100, or 200 ms. They are fed to the computer and low-pass filtered. The relationship between gravity and the output voltage of the sensor is expressed by

$$g=k_1\tilde{V}+k_2\ ,$$

where k_1 and k_2 are constants, $\tilde{V}$ is a smoothed voltage output. Smoothing of the ship's disturbing acceleration is conducted by using a digital filter. What is different from the case of NIPR-ORI Model I is the quicker sampling of the data and the longer time constant of the weight function. The weight function used here is also of the error function type, which is expressed by

$$\phi(t)=\frac{1}{\sqrt{2\pi}\,\sigma}e^{-\frac{t^2}{2\sigma^2}}\ ,$$

whose Fourier transform is expressed by

$$F(t)=\frac{1}{\sqrt{2\pi}}e^{-\frac{\sigma^2\omega^2}{2}}\ .$$

This weight function shows a very strong filtering effect for noises whose period is shorter than σ seconds. σ was taken 30 s in the previous case. However, with this weight function, filtering becomes very weak when the period of noises is longer than σ seconds. The change of filter effectiveness at the border of σ is very sharp. It is well known that the ship's acceleration noises are generally of the wide band, longer period change of acceleration being recognized, which is caused mostly by yawing motion. So, in the present processing, σ is set 60, 90 and 120 s and used selectively. Navigational data can be taken in real time, and the Eotvos and Bouguer corrections, free air and Bouguer anomalies based on the normal gravity can be obtained also in real time. These values are printed, stored in the hard disc and the magnetic tapes. Gravity values are calculated at any interval selected from among 1 min to multiples of minute.

8. Test of Performance

The first test on the performance of the NIPR-ORI gravimeter Model II was conducted on board R/V HAKUHO MARU of the Ocean Research Institute, University

of Tokyo from 1 July to 13 August 1987. The area of the test measurement is the Philippine Sea. The ship cruised from Tokyo down to the area of 9°N. Since this is the first test of the gravimeter the sensitivity k_1 and k_2 were still uncertain. These values were determined using three calibration points, where the ship was moored, *i.e.*, Harumi pier of Tokyo, Victor No. 6 Pier of Apra inner harbor, Guam and a pier of Colonia district, Island of Yap (Federated States of Micronasia). At each pier gravity was measured by a LaCoste & Romberg Land Gravimeter (Model G, No. 124) and the gravity at the level where the sea gravimeter was placed was estimated. In this case the drift rate of the sea gravimeter and the effect from the ambient temperature have also to be taken into account. So, gravity and sensor signal relationship is rewritten as

$$g=k_1\tilde{V}+k_2+k_3t+k_4\Delta T\,,$$

where k_3 is the drift rate (mgal/day), k_4 the temperature co-efficient, t the period of measurement in days and ΔT the ambient temperature difference with respect to reference temperature. By using this formula and applying gravity at the three piers the constants k_1, k_2, k_3 and k_4 were determined by the least squares method. The results are shown in Table 3. The differences of measured gravity (NIPR-ORI—LaCoste) at the piers are plotted in Fig. 14 as a function of days.

Table 3. Gravity formula to be applied to NIPR-ORI gravimeter Model II.

k_1:	0.03271226	$\pm$0.00003478	mgal/μV
k_2:	979712.5	$\pm$1.66	mgal
k_3:	−0.62922	$\pm$0.05550	mgal/day
k_4:	−1.331	$\pm$0.05	mgal/°C

$[g=k_1\tilde{V}+k_2+k_3t+k_4\Delta T]$

g: Gravity in mgal.
$\tilde{V}$: Voltage output from gravimeter in μV.
t: Time elapsed in days.
ΔT: Change in ambient temperature in °C.
k_1: Gravity scale factor in mgal/μV.
k_2: Gravity bias in mgal.
k_3: Gravity drift mgal/day.
k_4: Temperature co-efficient of gravity in mgal/°C.

Figure 15 shows an example of the raw gravity profile measured at the interval of 1 min. It is found that the measurement was performed well. In this measurement the ship's movement was of the amplitude of about 50 gal.

During the test measurement there were five crossings of the ship's tracks where two measurements at the same points were compared. This comparison could not be made straightforwardly because of the ambiguity of the position for crossings: NNSS fixes and Loran C fixes do not agree and in some places either of the two is lacking. In Table 4 the absolute values of the differences between two measurements at the crossings are summarized. Gravity at crossings determined by NNSS agrees within the accuracy of 1.6 mgal on an average, while those at crossings determined by Loran C are diversified to the order of magnitude of 9 mgal. There were two points of crossings (Nos. 2 and 5) where GPS was available for positioning. When the Eotvos corrections by GPS were applied we could get the differences of 0.4 and 0.7 mgal at points

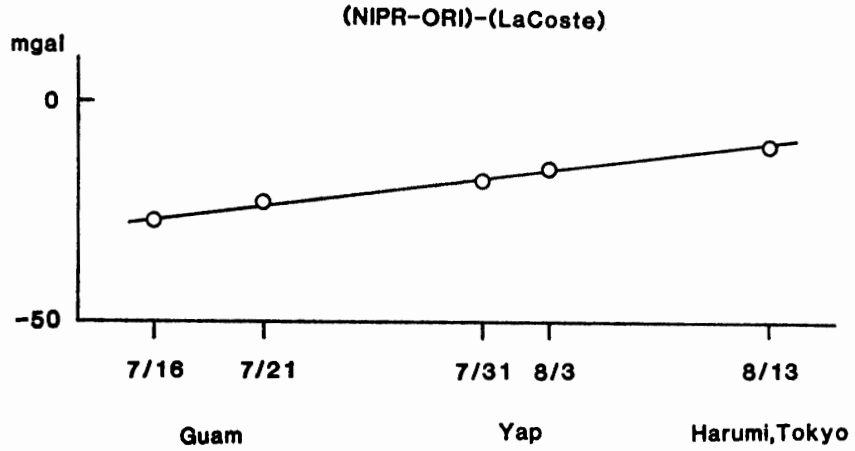

Fig. 14. Differences [NIPR-ORI minus LaCoste] at the piers visited (after temperature correction).

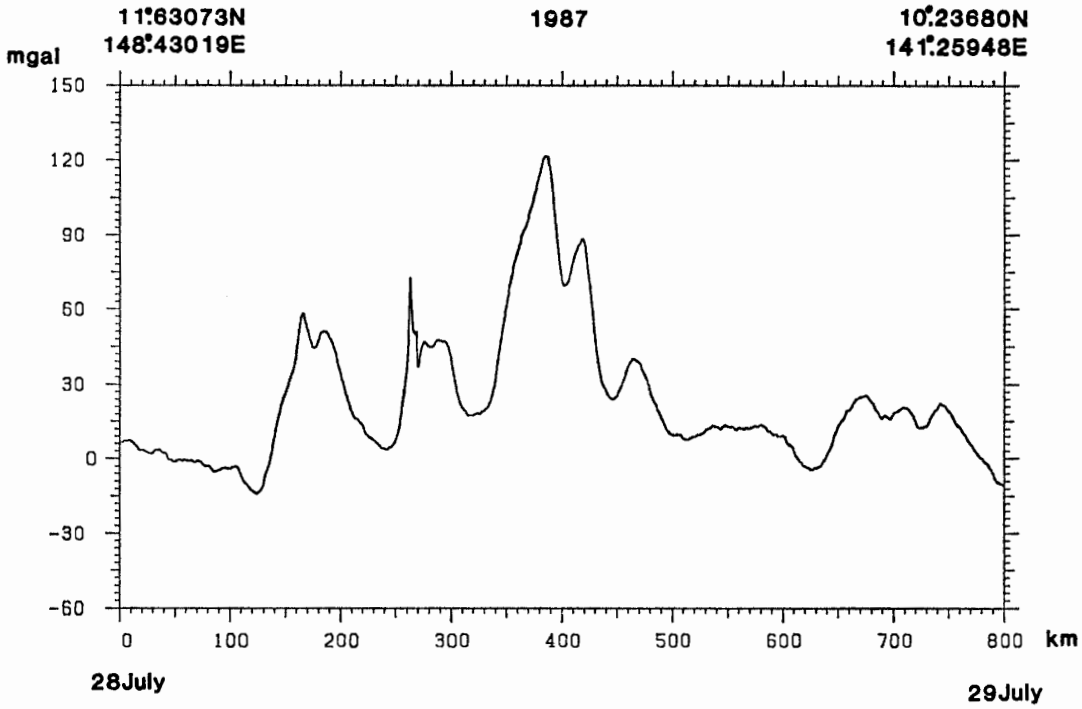

Fig. 15. An example of raw gravity profile measured at the interval of 1 min in the sea near Yap Island.

Table 4. Absolute values of differences between two measurements at crossover points numbered 1 through 5. The differences depend on the method of positioning (by NNSS or Loran C).

No. of crossover point	1	2	3	4	5	
Difference	1.8	1.5	—	0.6	2.8	(mgal) by NNSS
Difference	5.8	13.8	8.4	—	—	(mgal) by Loran
Difference	—	0.4	—	—	0.7	(mgal) by GPS

No. 2 and No. 5, respectively. In this estimation the Eotvos corrections were given from the rate of instantaneous position changes. This rate scattered widely with the case of Loran C fixes. The results of comparison of gravity at crossovers given here show that the accuracy of gravity measurements by the use of NIPR-ORI Model II is 0.5 mgal or better if a good navigational aid such as GPS is available.

Acknowledgments

We are grateful to the staff of the National Institute of Polar Research for their encouragement during the development of the gravimeter. We also thank Tokyo Keiki Company who undertook manufacturing the hardware. The crew of the R/V HAKUHO MARU kindly assisted us in the case of the test cruise.

References

KASUGA, T., FUCHINOUE, S., KAMINUMA, K. and SEGAWA, J. (1983): Sea gravity measurements in the Antarctic regions during the 22nd and 23rd Japanese Antarctic Research Expeditions. Mem. Natl Inst. Polar Res., Spec. Issue, **28**, 81–92.

SEGAWA, J., KASUGA, T. and KAMINUMA, K. (1983): Surface ship gravity meter NIPR-ORI I. Mar. Geod., **7**, 271–290.

SEGAWA, J., KAMINUMA, K. and FUKUDA, Y. (1986): Processing of sea gravity data using on-line navigational information of icebreaker SHIRASE. Mem. Natl Inst. Polar Res., Spec. Issue, **43**, 13–18.

(Received June 1, 1988; Revised manuscript received October 5, 1988)